rd1 Photoreceptor Degeneration: Photoreceptor Rescue and Role of Metalloproteases in Retinal Degeneration

Ahuja Jensen, Poonam

2005

Neuroscience 131 (2005) 935–943

DECREASED GLUTATHIONE TRANSFERASE LEVELS IN rd1/rd1 MOUSE RETINA: REPLENISHMENT PROTECTS PHOTORECEPTORS IN RETINAL EXPLANTS

P. AHUJA, A. R. CAFFÉ,* S. AHUJA, P. EKSTRÖM AND T. VAN VEEN

Wallenberg Retina Centre, Department of Ophthalmology, Lund University, BMC-B13, Klinikgatan 26, Lund 221 84, Sweden

Abstract—Currently much attention is focused on glutathione S transferase (GST)-induced suppression of apoptosis. The objective of our studies was therefore to see if GST isoenzymes rescue photoreceptors in retinal explants from *rd1*/*rd1* mice, in which photoreceptors degenerate rapidly. Eyes from C3H *rd1*/*rd1* and +/+ mice were collected at various time points between postnatal day (PN) 2 and PN28. Localization and content of α-GST and μ-GST was investigated by immunofluorescence and semi-quantitative Western blot analysis, respectively. In addition, PN2 and PN7 retinal explants were cultured till PN28, during which they were treated with 10 ng/ml α-GST or μ-GST. The spatiotemporal expression of both GST isoforms was closely similar: early presence in ganglion cell layer after which staining became restricted to Müller cells (particularly in the endfeet) and horizontal cell fibers in both *rd1*/*rd1* and +/+. Doublets of α-GST and μ-GST were detected by Western blot analysis. Densitometry of these bands indicated steady reduction of α-GST content in *rd1*/*rd1* retina starting from the second postnatal week. When α-GST and μ-GST were added exogenously to *rd1*/*rd1* explants, photoreceptor rescue was produced that was more prominent in PN2 than in PN7 explants and more effective by α-GST than μ-GST. We propose that α-GST neuroprotection is mediated by reduction of tissue oxidative stress. © 2005 Published by Elsevier Ltd on behalf of IBRO.

Key words: GST, neuroprotection, retinal degeneration, culture.

The *rd1*/*rd1* mouse has an insertion of viral DNA in the β-subunit of the cGMP phosphodiesterase gene (Bowes et al., 1990; Pittler and Baehr, 1991). This leads to a total degeneration of rods between postnatal day (PN) 7 and PN21 leaving only a single layer of cones in the outer nuclear layer (ONL) of the retina (Sanyal and Bal, 1973; Carter-Dawson et al., 1978). Subsequently remaining cones also die. Defects in the same gene are involved in human forms of retinitis pigmentosa (McLaughlin et al., 1995) and, for this reason the *rd1*/*rd1* mouse serves as an adequate model for human inherited retinal degenerative disease. Use of an *in vitro* mouse retinal explant assay, such as the one we and others have developed (Caffé et al., 1989, 2001a; Caffé and Sanyal, 1991; Mosinger-Ogilvie et al., 1999), allows screening of potential therapeutic factors for retinal degenerative disease under rigidly controlled conditions. Previously combinations of nerve growth factor and fibroblast growth factor-2 as well as ciliary neurotrophic factor (CNTF) and brain-derived neurotrophic factor (BDNF) have been shown to retard *in vitro* loss of *rd1*/*rd1* photoreceptors (Caffé et al., 1993, 2001b; Mosinger-Ogilvie et al., 2000). Lately we reported that lens epithelium-derived growth factor (LEDGF) also retards *rd1*/*rd1* photoreceptor loss in culture when compared with untreated tissue (Ahuja et al., 2001).

Apart from these typical growth factors, other classes of compounds might be of benefit in attempts to retard neurodegeneration. For instance, supplementation of glutathione peroxidase, thioredoxin, superoxide dismutase, or catalase and their synthetic mimetics, to growth medium may protect neurons or retinal pigment epithelium (RPE) cells *in vitro* (Lipton et al., 1993; Akeo et al., 1996; Castagné and Clarke, 2000). All of these are redox-regulating enzymes. However, their neuroprotective effect may be independent from their involvement in redox regulation. Such an example is glutathione S transferase (GST). A series of recent studies have shown that several forms of GST isoenzymes interact with different protein kinases in stress-induced pathways thus indicating that GST isoenzymes might play an additional role at the level of cellular signaling and regulation. A number of cytosolic GST isoenzymes have been purified from vertebrate organs. On the basis of their primary structure cytosolic GST isoenzymes are divided into five families designated class α-, μ-, π-, σ-, and θ-GST (Hayes and Pulford, 1995). Intracellular π-GST interacts with c-Jun N-terminal kinase (JNK), whereas μ-GST and thioredoxin interact with and inhibit apoptosis signal-regulating kinase 1, which modulates the two downstream JNK and p38 mitogen-activated protein kinase apoptotic pathways and inhibits or deactivates them (Adler et al., 1999; Cho et al., 2001). The p38 apoptotic pathway has been linked directly to *rd1*/*rd1* retinal degeneration (Jomary et al., 2001). Usually intracellular GST levels change after trauma or during pathology (Mannervik and Danielson, 1988; Lovell et al., 1998), in agreement with reports that investigated this issue in retina (McGuire et al., 1996, 2000). But, whether this also happens during *rd1*/*rd1*

*Corresponding author. Tel: +46-46-222-0767; fax: +46-46-222-0774.
E-mail address: romeo.caffe@oft.lu.se (A. R. Caffé).

Abbreviations: BDNF, brain-derived neurotrophic factor; CNTF, ciliary neurotrophic factor; div, days *in vitro*; ECL, enhanced chemiluminescence; FITC, fluorescein isothiocyanate; GCL, ganglion cell layer; GS, glutamine synthetase; GST, glutathione S transferase; H&E, hematoxylin and eosin; JNK, c-Jun N-terminal kinase; LEDGF, lens epithelium-derived growth factor; ONL, outer nuclear layer; OPL, outer plexiform layer; PBST, phosphate-buffered saline Triton X-100; PN, postnatal day; ROS, reactive oxygen species; RPE, retinal pigment epithelium; RT, room temperature; TBST, Tris-buffered saline plus Triton X-100.

0306-4522/05$30.00+0.00 © 2005 Published by Elsevier Ltd on behalf of IBRO.
doi:10.1016/j.neuroscience.2004.11.012

retinal degeneration was unknown. Therefore we studied the following questions: (1) if tissue level of GST changes during *rd1*/*rd1* retinal degeneration; (2) whether exogenous GST can also delay *rd1*/*rd1* photoreceptor loss *in vitro*.

Here we present evidence that both α- and μ-GST isoenzymes, the most abundant forms of GST, levels decrease from the second postnatal week of *rd1*/*rd1* retinal degeneration. Furthermore, exogenous α-GST and μ-GST can indeed rescue photoreceptors in *rd1*/*rd1* mouse retinal explants.

EXPERIMENTAL PROCEDURES

Animals

All experimental treatments were according to NIH guidelines and the European Communities Council Directive (86/609/EEC). The Swedish National Animal Care and Ethics Committee also approved the experiments. Homozygous retinal degeneration 1 (*rd1*/*rd1*) and congenic control (+/+) mice of the C3H strain from our own colonies were used. Day of birth was considered as PN0. Pups from PN2 and PN7 age were decapitated whereas older mice (PN14, PN21 and PN28) were killed by asphyxiation on dry ice. Efforts were made to minimize the number of animals used and their suffering.

Detection and semi-quantification of α- and μ-GST in retinal extracts by Western analysis

The *in vivo* retinas from two animals in each category were taken from PN2, PN7, PN14, PN21 and PN28 +/+ and *rd1*/*rd1* mice. After enucleating the eyes, the anterior segment, vitreous body, sclera and choroids were removed in the dissecting medium and retinas with RPE were frozen at −80 °C until used. Two retinas of the same kind were pooled and homogenized by hand in homogenizing buffer (2% sodium dodecyl sulfate, 10% glycerol and 62.5 mM Tris [pH 6.8]); the homogenate was centrifuged at 10,000 r.p.m. for 5 min. Protein concentration of the soluble particulate free supernatant was determined by using PlusOne 2-D Quant Kit (Amersham Biosciences, Uppsala, Sweden). Five micrograms of protein was loaded in each well and fractionated (Laemmli, 1970) in a discontinuous SDS–polyacrylamide gel (3% stacking gel, 12.5% separation gel) in a Mini-PROTEAN II apparatus (Bio-Rad Laboratories, Hercules, CA, USA). Molecular weight markers were of broad range biotinylated SDS-PAGE standards (Bio-Rad Laboratories) and *E. coli* produced human recombinant α-GST (62.5 ng) or μ-GST (50 ng; Oxford Biomedical Research, Oxford, MI, USA) served as molecular weight markers and positive reference protein, respectively. Proteins from the gel were transferred using a Semi-Dry blotter (Sammy Dry; Tamro Laboratories, Schleicher & Schuell, Bioscience GmbH, Dassel, Germany) on to polyvinylidene difluoride membranes (Immobilon-P; Millipore, Bedford, MA, USA) using blotting buffer (48 mM Tris base, 39 mM glycine, 0.0375% SDS, 20% methanol). The membranes were blocked for 1 h in Tris-buffered saline containing 0.1% Triton X-100 (TBST) and 5% skim milk (pH 7.2). This was followed by overnight incubation at 4 °C with either of the antibodies (1) anti-rat GST Ya (goat polyclonal; 1:10,000) that detects α-GST or (2) anti-rat GST Yb (goat polyclonal; 1:10,000) that detects μ-GST (Oxford Biomedical Research, Inc.). After 3×5 min rinse the membrane was incubated for 60 min with 1:10,000 HRP-conjugated donkey anti-goat (Scandinavian Diagnostic Services, Falkenberg, Sweden) at room temperature (RT) followed by 3×5 min washes in TBST. The immune complexes were visualized by enhanced chemiluminescence (ECL; Amersham Biosciences) on to X-ray film (Hyperfilm ECL; Amersham Biosciences). The intensity of each band was compared after semiquantification by optical densitometry (BIO-1D Software; Vilber Lourmat, Marne-La-Vallec Cedex, France). Experiments were performed in triplicate.

Development of μ- and α-GST in mouse retina

Eyes of same age groups used for Western blot were also used to perform cellular localization of GST isoenzymes in retina. After enucleation, eye cups were fixed in cold 4% paraformaldehyde for 1 h, cryoprotected and cut at 8-μm thickness on a cryostat. A few sections were stained with hematoxylin and eosin (H&E) and others subjected to immunofluorescence studies. Primary antibodies were: (1) anti-rat GST Ya (goat polyclonal; 1:500) that detects α-GST; (2) anti-human GST M1-1 (rabbit polyclonal; 1:500) that detects μ-GST (Oxford Biomedical Research, Inc.), diluted in phosphate-buffered saline (pH 7.2) containing 1% bovine serum albumin and 0.25% Triton X-100 (PBST). Sections were pre-incubated with PBST for 30 min at RT followed by overnight incubation with the diluted primary antibody at 4 °C. In case of negative control sections the primary antibodies were omitted. After washing with PBST for 3×5 min, bound primary antibody was detected by incubation with rabbit anti-goat conjugated to fluorescein isothiocyanate (FITC) or goat anti-rabbit antibody conjugated to FITC (DAKO, Glostrup, Denmark; 1:200). After another wash with PBST for 3×5 min each, the slides were mounted with Vectashield anti-fade medium (Vector Laboratories, Burlingame, CA, USA).

To confirm the identity of stained profiles double labeling of GST M1-1 with either glutamine synthetase (GS; mouse monoclonal, 1:100; Chemicon, Temecula, CA, USA) or neurofilament (mouse monoclonal, 1:3000; Sigma, St. Louis, MO, USA) was performed on PN28 +/+ retina. The second secondary antibody used in both the cases was Alexa Fluro 589 goat anti-mouse (Molecular Probes, Eugene, CA, USA; 1:200). For double labeling, sections were initially incubated with the first primary antibody overnight followed by the first secondary antibody and then again overnight with the second primary antibody followed by the second secondary antibody. Washes with PBST were performed in between each step as described above.

Immunohistochemical labeling was examined and documented using an Axiophot photomicroscope (Zeiss, Oberkochen, Germany). Adobe Photoshop was used for image processing. Only contrast and brightness of images was adjusted. In the double labeling experiments separate digital images of the fluorophores were superimposed on each other, resulting in a yellow or orange signal depending on the intensity in case of co-localization.

Long-term α-GST and μ-GST treatment of retinal explants to study the rescue effect

PN2 and PN7 retinas were used to generate mouse retinal explants from *rd1*/*rd1* and +/+ animals as described before (Ahuja et al., 2001). The incubation medium was supplemented with either 10 ng/ml of human recombinant α-GST, μ-GST (Oxford Biomedical Research, Inc.) or vehicle as a control. According to the data sheets specific activity of α-GST was 57 μmol/min/mg using spectrophotometric determination of 1-chloro-2,4-dinitrobenzene conjugation with reduced glutathione (1 mM) in 100 mM $K3PO_4$, pH 6.5 at RT, while that of μ-GST was 207 μmol/min/mg with 10 mM reduced glutathione. For long-term incubation studies all explants were cultured till the age of PN28; meaning that PN2 and PN7 explants were kept for 26 and 21 days *in vitro* (div), respectively. At the end of culture period the retinal explants (PN2+div26 and PN7+div21) attached to the carrier membrane were fixed and processed according to the protocol described for immunocytochemistry. A number of sections were stained with H&E to study morphology and to count the number of photoreceptor rows in ONL. For the latter a vertical column in the center of the retina was chosen and a previously described counting

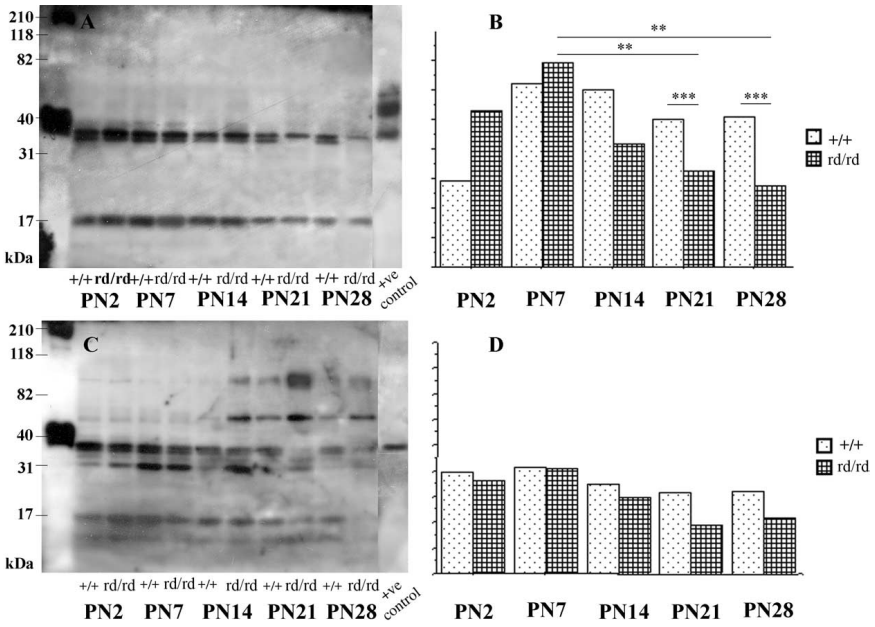

Fig. 1. Western analysis demonstrating age dependent levels of α-GST and μ-GST levels in +/+ and rd1/rd1 retinas. Panels A and B display the Western blot and semi-quantification of α-GST, respectively. The Western blot shows a doublet co-migrating with recombinant α-GST protein. The densitometry of the α-GST bands shows that between PN2 and PN7 a development increase in levels of this protein is observed in both +/+ and *rd1*/*rd1* retinal extracts. Note that from PN7 to PN28 no major alterations in levels of this protein occur in the +/+ retina. In contrast, in the *rd1*/*rd1* retina levels dramatically decrease after PN7 with changes being statistically significant ($P<0.01$). Both at PN21 and PN28 levels in *rd1*/*rd1* were also statically significantly reduced compared with age-matched +/+. Panels C and D illustrate similar data for μ-GST. The Western blot shows a band co-migrating with recombinant μ-GST protein. Densitometry of the μ-GST bands shows that from PN2 to PN28 no statistically significant alterations in levels in +/+ as well as *rd1*/*rd1* retinas occur, although in the *rd1*/*rd1* retina the levels displayed a tendency to decrease after PN7. ** $P<0.01$; *** $P<0.001$.

procedure was followed (Caffé et al., 1993). All data are presented as mean±S.E.M. Data were analyzed using one way analysis of variance at 5% significance level, followed by Fisher's protected least significant difference post hoc comparisons. The difference between groups was regarded as significant if $P<0.05$.

RESULTS

α-GST levels are decreased in *rd1*/*rd1* mouse retina

Fig. 1A, B display Western blots and statistical analysis, respectively, obtained for α-GST. Western analysis revealed that the antibody reacted with a band migrating at approximately 17 kDa and a doublet co-migrating with the positive control at approximately 35 kDa (Fig. 1A). This latter doublet was regarded as the protein(s) of interest and scanned for statistical analysis of which results were plotted in Fig. 1B. This graph showed that in *rd1*/*rd1* retinal extract α-GST content increased between PN2 and PN7, after which levels declined starting at a time point between PN7 and PN14. This decline continued till PN28, the last measured time point. The difference in α-GST levels between PN7 and PN21 as well as between PN7 and PN28 in *rd1*/*rd1* retina was statistically significant ($P<0.01$). By contrast, after having reached peak levels during the second postnatal week, α-GST levels remained stable in +/+ retinal extracts and no statically significant differences occurred during 4 weeks of retinal maturation. From PN14 onwards α-GST levels were significantly reduced in *rd1*/*rd1* retina compared with +/+ counterparts (Fig. 1B).

Fig. 1C, D display Western blots and numerical data, respectively, obtained for μ-GST. Western analysis revealed several protein bands migrating at approximately 17 kDa, approximately 31 kDa and approximately 60 kDa, but a doublet co-migrating with the positive control at approximately 37 kDa (Fig. 1C) was regarded as the protein(s) of interest and used for statistical analysis. The results showed that in *rd1*/*rd1* retinal extract μ-GST levels had the tendency to decrease after PN7, but this effect was not statistically significant. In +/+ retina μ-GST levels remained stable during retinal maturation. At none of the studied time points μ-GST level was significantly reduced in *rd1*/*rd1* retina compared with the +/+ counterpart (Fig. 1D).

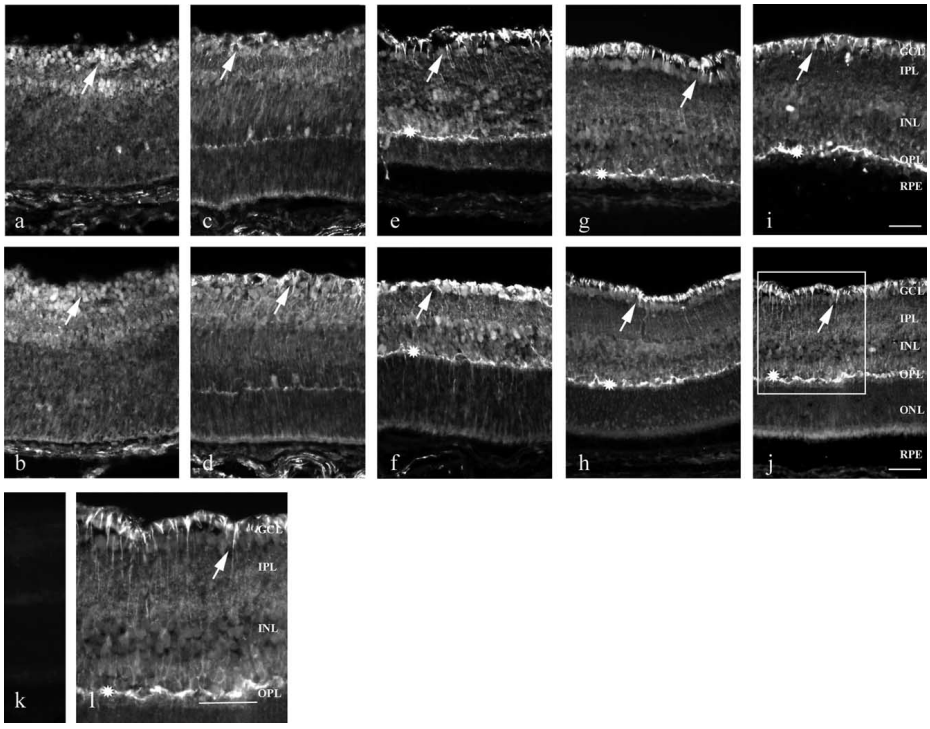

Fig. 2. Immunostaining of mouse retina for α-GST at different postnatal ages in vivo. Panels in the top row show examples of PN2 (a), PN7 (c), PN14 (e), PN21 (g), and PN28 (i) *rd1*/*rd1* stained retinal sections whereas panels in the bottom row illustrate corresponding +/+ retinal sections. At PN2 (a, b) and PN7 (c, d) *rd1*/*rd1* retinas as well as their +/+ counterparts show α-GST immunoreactivity (IR) in the GCL region suggestive of intracellular neuronal presence of α-GST (arrow). In addition, at PN7 weak labeling in presumptive horizontal cell bodies and their processes can be observed. In PN14 *rd1*/*rd1* retinal sections (e), α-GST IR in neuronal profiles of GCL is much reduced and replaced by an immunopattern indicative of stained Müller cell endfeet and perhaps astrocytes (arrow). Additionally, strong expression persists at the level of the OPL (asterisk). The age-matched +/+ counterpart (f) shows a similar staining pattern as *rd1*/*rd1* tissue in the GCL (arrow) as well as the OPL (asterisk). In both *rd1*/*rd1* (g) and +/+ (h) retinal sections from PN21 α-GST expression in the GCL is now clearly restricted to presumptive Müller cell endfeet (arrows) and in the OPL (asterisks). With further maturation at PN28, Müller cell endfeet and OPL staining persist (arrows, asterisks). Panel k, negative control showing absence of IR after only the secondary goat antibody is applied. Panel l is higher magnification of panel j showing distinct α-GST labeling in the Müller cells radial endfeet and descending processes (arrow) and also in the horizontal oriented fibers in the OPL (asterisk). Scale bar=50 μm.

α- And μ-GST are localized in Müller cells and horizontal cell fibers of *in vivo* retina

Cellular expression of α- (Fig. 2) and μ-GST (Fig. 3) showed closely similar spatiotemporal developmental pattern and, therefore, will be presented together. At PN2, when there was no morphological difference in retinal structure between *rd1*/*rd1* and +/+ genotypes, weak expression of both GST isoforms was detected in developing ganglion cell layer (GCL; Figs. 2a, b; 3a, b; arrow). Labeling of astrocytes could not be excluded. At PN7 labeling for both GST isoforms was still prevalent in GCL region, but contours of Müller cell endfeet and profiles at the developing inner limiting membrane became better discernable along with presentation of weak-immunoreactivity in developing horizontal cells (Figs. 2c, d; 3c, d; arrow). Between PN7 and PN14 rod degeneration got under way in *rd1*/*rd1* mouse retina, while in *wt* retina photoreceptors underwent further differentiation. At PN14 both α- and μ-GST are now clearly detectable in Müller cell endfeet including the descending trunks of the radial processes as well as fibers coursing horizontally in the outer plexiform layer (OPL; Figs. 2e, f; 3e, f; arrow). After PN14 both GST isoform staining patterns in *rd1*/*rd1* developed different characteristics from those in +/+ genotypes, in particular for α-GST. From PN21 to PN28 α- and μ-GST immunoreactivity in Müller cell endfeet and fibers in OPL persisted throughout development (Fig. 2g, i; Fig. 3g, i).

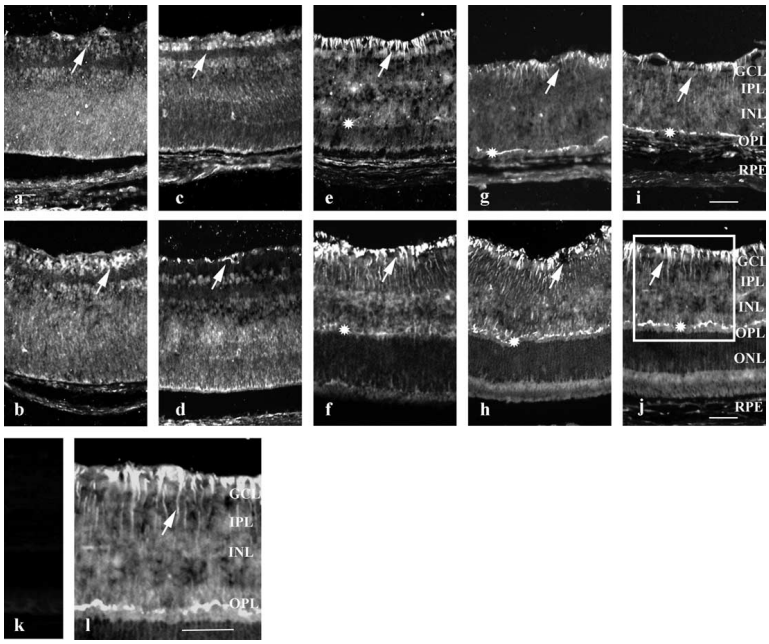

Fig. 3. Immunostaining of mouse retina for μ-GST at different postnatal ages *in vivo*. Top row images show photomicrographs from PN2 (a), PN7 (c), PN14 (e), PN21 (g), and PN28 (i) *rd1*/*rd1*-stained retinal sections whereas panels in the bottom row illustrate corresponding +/+ retinal sections. At PN2 (a, b) as well as PN7 (c, d) both *rd1*/*rd1* and +/+ retinas show μ-GST IR in the GCL region suggestive of intracellular neuronal presence of this enzyme (arrow, a–c). However, clear presumptive glial elements are also observed to express staining at PN7 in +/+ tissue (d, arrow). At the PN14 age *rd1*/*rd1* (e) as well as +/+ (f) retinal sections exhibit clear μ-GST IR in Müller cell endfeet (arrow), while some labeling emerges in the OPL (asterisk). Additionally, strong expression persists at the level of the OPL (asterisk). At PN14 (e, f), PN21 (g, h), and PN28 (i, j), Müller cell endfeet (arrow) and OPL staining (asterisk) persist. Panel k, negative control showing absence of IR after only the secondary goat antibody is applied. Panel l is higher magnification of panel j showing distinct μ-GST labeling in the Müller cells radial endfeet and descending processes (arrow) and also in the horizontal oriented fibers in the OPL (asterisk). Scale bar=50 μm.

To unambiguously confirm presence of GST immunoreactivity in Müller and horizontal cells retinal sections were double-labeled using antibodies against GST M1-1 combined with either GS or neurofilament. Fig. 4a–c displays μ-GST (Fig. 4a), neurofilament (Fig. 4b) and the superimposed image (Fig. 4c). The results demonstrated co-localization of μ-GST and GS, thereby confirming presence of GST in Müller cell endfeet (arrows) and radial processes. Staining of astrocytes could not be excluded. Fig. 4e–g depicts μ-GST (Fig. 4e), neurofilament (Fig. 4f), and the superimposed image (Fig. 4g). This showed co-localization of μ-GST and neurofilament, thereby confirming presence of GST in fibers extending from horizontal cells (arrowheads).

α- and μ-GST treatments rescue photoreceptors in PN2 *rd1*/*rd1* mouse retinal explants

PN2 or PN7 retinal explants were cultured with or without α-GST or μ-GST supplementation to the medium and analyzed at PN28. Without these factors PN2+div26 *rd1*/*rd1* retinal explants displayed 2.6±0.1 rows of nuclei in ONL (Fig. 5c, Fig. 6). Similar tissue treated with α-GST showed 4.6±0.2 rows of nuclei (Fig. 5a, Fig. 6) and when treated with μ-GST showed 4.7±0.2 rows of nuclei (Fig. 5b, Fig. 6). In both treated cases a rescue effect was found that was significant at $P<0.01$ (Fig. 6). Corresponding PN2+div26 +/+ retinal explants exhibited 7.3±0.2 rows of nuclei in the ONL (Fig. 5f, Fig. 6), which was not different statistically from α-GST- (Fig. 5d, Fig. 6) and μ-GST- (Fig. 5e, Fig. 6) treated tissue, which had 7.1±0.1 rows of nuclei and 7.2±0.1 rows of nuclei respectively (Fig. 6). A rescue effect of α-GST and μ-GST, although less pronounced, was also observed in PN7+div21 *rd1*/*rd1* tissue. The responses of untreated PN7+div21 *rd1*/*rd1* (Fig. 5i, Fig. 6) explants displayed 2.3±0.2 rows of nuclei in the ONL, whereas similar tissue treated with α-GST (Fig. 5g, Fig. 6) showed 3.1±0.1 rows of photoreceptor and that treated with μ-GST (Fig. 5h, Fig. 6) showed 2.7±0.2. Only α-GST

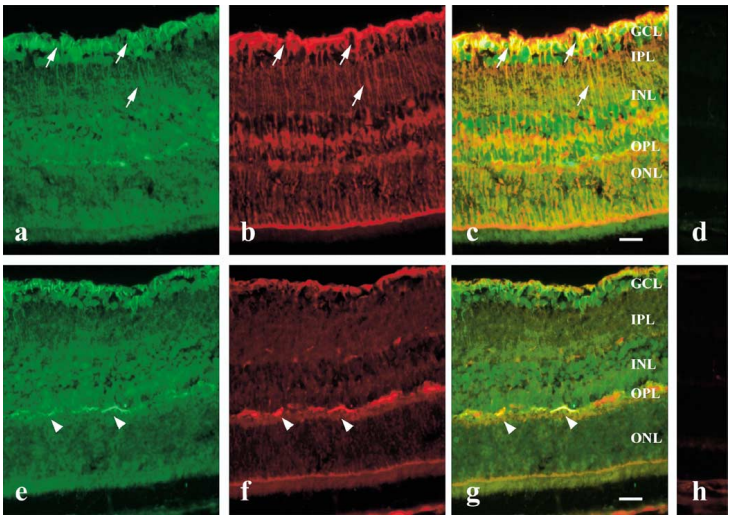

Fig. 4. μ-GST IR retinal profiles in the in vivo retina identified as Müller cell and horizontal cell fibers. All sections are derived from PN28 +/+ *in vivo* retina. Panels a–c display the μ-GST (a), GS (b), and the superimposed image (c). Co-localization of μ-GST and GS is observed in Müller cell endfeet (arrow) and radial processes. Panel d, negative control showing absence of IR after only the secondary antibodies are applied. Panels e–g depict the μ-GST(e), neurofilament (f), and the superimposed image (g). Co-localization is present in the horizontal oriented fibers in the ONL (arrowhead). Panel h, negative control showing absence of IR after only the secondary antibodies are applied. Scale bar=50 μm.

treatment was significant at the $P<0.05$ level (Fig. 6) when compared with the untreated one. Untreated PN7+div21 +/+ explants were not statistically different from α-GST- and μ-GST-treated ones (Fig. 6). The PN7+div21 +/+ untreated (Fig. 5l, Fig. 6) showed 8.0±0.2 rows as compared with α-GST (Fig. 5j, Fig. 6) which showed 7.1±0.1 rows of nuclei and μ-GST treated (Fig. 5k, Fig. 6) which showed 7.2±0.1 rows of nuclei. The rescue effect by α-GST and μ-GST on *rd1*/*rd1* explants at PN2+div26 was significantly higher than the effect at PN7+div21 (Fig. 6).

DISCUSSION

Anatomical localization of GST isoenzymes in mouse retina: endogenous GST isoenzymes act as detoxifying agents

Intracellular detoxification is supposedly the most important function of cytoplasmic GST isoenzymes (see Hayes and Pulford, 1995; Salinas and Wong, 1999). The anatomical localization of various GST isoenzymes has been investigated previously in rat retina. Results demonstrate that the μ-GST is primarily present in Müller cells and photoreceptor outer segments, the α-GST is found in Müller cells, whereas amacrine cells express staining after using antisera directed against π-GST (Ahmad et al., 1988; Singh et al., 1984; Naash et al., 1988; McGuire et al., 1996). We have found α- and μ-GST immunolabeling in Müller cell endfeet and, interestingly, in large caliber horizontal cell fibers. A common denominator between A-type (axonless) horizontal cells and Müller cell endfeet is that they contribute to the formation of the inner blood–retinal barrier composed of the deep capillary layer of retina at the OPL and the superficial retinal capillary layer at the inner limiting membrane (Knabe and Ochs, 1999; Yu and Cringle, 2001). We suggest that GST isoenzymes can be secreted, as has been shown in tissues such as the seminiferous tubules (Mukherjee et al., 1999). The GST staining in the retinal OPL is, thus, strategically positioned to protect retina against toxic molecules that penetrate from the blood retinal capillaries into the retinal syncytium. In order to further support this hypothesis GST stainings as done here should be performed in partially vascularized retinas like those from rabbit and horse and avascular retinas as that from the guinea-pig (but see Pow and Crook, 1995). Alternatively, Müller cells and the horizontal cells are in appropriate positions to release GST molecules which could then interact with reduced glutathione and proteins on the surface of photoreceptors and presumably influence their survival. Curiously, GST isoenzymes have been shown to bind to steroids such as estrogens and these steroids have a potent effect on photoreceptor survival in a variety of retinal degeneration models (Yu et al., 2004).

Lower α-GST levels in *rd1*/*rd1* as compared with +/+ retina

GST doublets in Western blot migrated slightly above the reference protein because the latter is a recombinant pro-

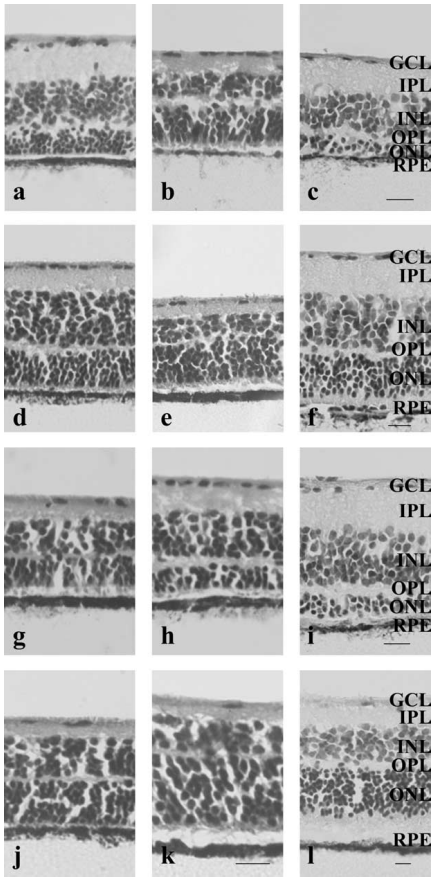

Fig. 5. α-GST and μ-GST rescues photoreceptor cell in rd1/rd1 mouse retinal explants. Photomontage demonstrating H&E-stained sections of mouse retinal explants from the following experimental conditions: (a) PN2+div26 *rd1*/*rd1* α-GST treated. (b) PN2+div26 *rd1*/*rd1* μ-GST treated. (c) PN2+div26 *rd1*/*rd1* untreated. (d) PN2+div26 +/+ α-GST treated. (e) PN2+div26 +/+ μ-GST treated. (f) PN2+div26 +/+ untreated. (g) PN7+div21 *rd1*/*rd1* α-GST treated. (h) PN7+div21 *rd1*/*rd1* μ-GST treated. (i) PN7+div21 *rd1*/*rd1* untreated. (j) PN7+div21 +/+ α-GST treated. (k) PN7+div21 +/+ μ-GST treated. (l) PN7+div21 +/+ untreated. It shows that PN2+div26 *rd1*/*rd1* untreated explants contain two rows whereas similar α-GST- and μ-GST-treated explants display five rows in the ONL (ONL thicker in a and b than in c). PN2+div26 +/+ treated and untreated explants remain unaffected in this respect. Panels g and h show that PN7 *rd1*/*rd1* retinal explants are less responsive to μ-GST treatment compared with PN2 *rd1*/*rd1* explants. Scale bar=25 μm.

tein and thus non-glycosylated whereas the GST in the tissue is glycosylated. Various authors have reported either upregulation (McGuire et al., 2000) or downregulation (Lovell et al., 1998) of GST expression, protein content or activity in neural tissue exposed to an insult. The idea is that increased intracellular levels of GST signal attempts by the tissue to fight oxidative stress that can lead to cellular toxicity. Lower GST activities have been found primarily in end-stage disease. It is unclear whether intracellular GST first increases and then declines. Here we have observed that retinal GST levels are maintained, or even slightly increase, till late in the degenerative changes in the *rd1*/*rd1* retina, before these levels fall sharply. This supports the notion that GST behaves in a bimodal fashion. It is important to note that the observed decreased level in GST is not an artifact of photoreceptor cell loss since these cells do not express the GST protein. The decline is akin to that found in some brain regions affected by Alzheimer's disease (Lovell et al., 1998). An assessment of the significance of GST dynamics, as a superimposed risk to the *rd1*/*rd1* retinal degenerative process, can be inferred from the kinetics of loss of photoreceptors correlated to GST observed changes.

Exogenous α- and μ-GST isoenzymes act as extracellular antioxidants

Following experiments that evaluated neuroprotective effects from exogenous redox-regulating enzymes we have supplemented GST to *rd1*/*rd1* retinal explants. α- As well as μ-GST supplementation to the culture medium rescues

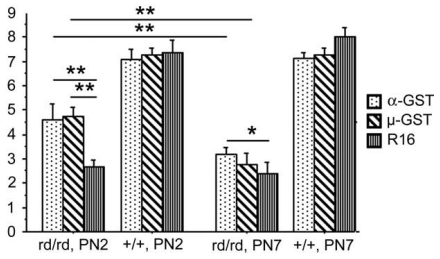

Fig. 6. Statistical analysis of α-GST and μ-GST effect in retinal explants. The data are presented as the number of rows (mean±SED) of nuclei in the ONL. Number of rows in PN2+div26 *rd1*/*rd1* untreated explants (2.6±0.1) is significantly different from that of both PN2+div26 *rd1*/*rd1* α-GST- (4.6±0.2) and PN2+div26 *rd1*/*rd1* μ-GST- (4.7±0.2) treated tissue, $P<0.01$. Number of rows in PN2+div26 +/+ untreated explants (7.3±0.2) is statistically not different from that of PN2+div26 +/+ α-GST-treated (7.1±0.1) and PN2+div26 μ-GST-treated tissue (7.2±0.1). Number of rows in PN7+div21 *rd1*/*rd1* untreated explants (2.3±0.2) is significantly different from that of PN7+div21 *rd1*/*rd1* α-GST-treated tissue (3.1±0.1), $P<0.05$. Number of rows in PN7+div21 +/+ untreated explants (8.0±0.2) is statistically not different from that of PN7+div21 +/+ α-GST-treated (7.1±0.1) and PN7+div21 +/+ μ-GST-treated tissue (7.2±0.1). The number of rows in the ONL of PN2+div26 *rd1*/*rd1* α-GST- and PN2+div26 *rd1*/*rd1* μ-GST-treated was also statistically significantly higher when compared with PN7+div21 *rd1*/*rd1* α-GST- and PN7+div21 *rd1*/*rd1* μ-GST-treated, $P<0.01$. In the PN2 and PN7 +/+ α-GST- and μ-GST-treated and untreated no statistically significant difference was seen. The rescue effect by μ-GST was more pronounced in the PN2+div28 explants compared with the PN7+div21 explants. ** $P<0.01$; * $P<0.05$.

rd1/*rd1* photoreceptors in the retinal explants and more efficiently so when cultures are started at PN2 age than at PN7. This rescue effect was not as potent as that found after CNTF and BDNF supplementation (Mosinger-Ogilvie et al., 2000; Caffé et al., 2001) but was similar to that seen after LEDGF application (Ahuja et al., 2001). There are three possible modes through which GST can affect retinal explants in order to rescue *rd1*/*rd1* photoreceptors. These include (1) uptake through the plasma membrane to act intracellularly; (2) binding extracellularly to transmembrane receptors; and (3) modulation of the extracellular environment. With regard to the first mode, no transmembrane receptors that recognize GST are known, although it has been reported that other redox regulating enzyme, i.e. extracellular superoxide dismutase, can bind to the cell surface via heparan sulfate proteoglycans (Karlsson et al., 1988). Evidence that GST can penetrate the cell membrane is also lacking. By deduction the site remaining for exogenously added GST to exert its rescue effect is likely to be the extracellular culture environment. This mode of action is not novel since other redox regulating enzymes like superoxide dismutase, catalase, and glutathione peroxidase or their synthetic mimetics exert either neuroprotective or neurodestructive effects when added to culture media (e.g. Oury et al., 1992; Bonfoco et al., 1995; Ricart and Fiszman, 2001). Our hypothesis is that exogenous GST, may also function as a peroxidase (Saneto et al., 1982; Singhal et al., 1999), thereby acting as an extracellular antioxidant similar to its function within the cell cytoplasm. It is often overlooked that in cell or tissue culture experiments the medium is present in a hyperoxic (95% O_2+5% CO_2) incubation atmosphere and due to this reactive oxygen species (ROS) may be produced (Leist et al., 1996; Halliwell et al., 2000; Grzelak et al., 2000). The tissue, especially when in a pathological state, is an additional source of ROS released into the culture medium (see Götz et al., 1994). Glutamate and dopamine receptors are among the retinal redox-sensitive cell surface receptors that enable this tissue to sense the extracellular redox state (e.g. Sucher and Lipton, 1991; Coyle and Puttfarcken, 1993; Tanaka et al., 2001). Based upon this line of thinking the differential sensitivity displayed between PN2 and PN7 retinal explant can be explained by the following arguments. First, the well-accepted molecular concept of an age-related decline in cellular response to oxidative stress (e.g. Holbrook and Ikeyama, 2002). Second, during maturation, physical changes like establishment of new neural circuits and activation-dependent events take place that induce functional changes like specialization of initial dual action receptors (e.g. Joseph et al., 1998; Puopolo et al., 2001). It is plausible that such maturational changes also occur in redox-sensitive receptor systems in the *rd1*/*rd1* retinal explant leading up to the differential response of PN2 and PN7 tissue to GST treatment. The observation that α-GST is more potent than μ-GST argues in favor of the redox-related function of GST isoenzymes since α-GST has more reductive power compared with μ-GST (Hayes et al., 1995). Validation of this extracellular antioxidant mechanism of GST-induced photoreceptor rescue will depends in part on supportive evidence generated by experiments whereby the redox-sensitive receptors are blocked.

Acknowledgments—The authors thank Birgitta Klefbohm, Hodan Abdalle and Katarzyna Said, Department of Ophthalmology, Lund University for taking care of the animals and technical help. Grant sponsors: Foundation Fighting Blindness USA, Dutch Retina Foundation, Crafoord Foundation, Crown Princess Margareta Foundation, Svenska Sallskapet for Medicinsk Forskning, Wallenberg Foundation, European Community Grant; PRO-AGE-RET: QLK6-CT-2001-00385 and 2nd ONCE international award for new technologies for the blind.

REFERENCES

Adler V, Zhimin Y, Fuchs SY, Benezra M, Rosario L, Tew KD, Pincus MR, Sardana M, Henderson CJ, Wolf CR, Davis RJ, Ronai Z (1999) Regulation of JNK signalling by GSTp. EMBO J 18:1321–1334.

Ahmad H, Singh SV, Medh RD, Ansari GAS, Kurosky A, Awasthi UC (1988) Differential expression of α, μ, and π classes of isozymes of glutathione S-transferase in bovine lens, cornea, and retina. Arch Biochem Biophys 266:416–426.

Ahuja P, Caffé AR, Holmqvist I, Soderpalm AK, Singh DP, Shinohara T, van Veen T (2001) Lens epithelium-derived growth factor (LEDGF) delays photoreceptor degeneration in explants of *rd1*/*rd1* mouse retina. Neuroreport 12:2951–2955.

Akeo K, Hiramitsu T, Kanda T, Karasawa Y, Okisaka S (1996) Effects of superoxide dismutase and catalase on growth of retinal pigment epithelial cells in vitro following addition of linoleic acid and linoleic acid hydroperoxide. Ophthalmic Res 28:8–18.

Bonfoco E, Krainc D, Ankarcrona M, Nicotera P, Lipton SA (1995) Apoptosis and necrosis: two distinct events induced, respectively, by mild and intense insults with *N*-methyl-D-aspartate or nitric oxide/superoxide in cortical cell cultures. Proc Natl Acad Sci USA 92:7162–7166.

Bowes C, Li T, Danciger M, Baxter LC, Applebury ML, Farber DB (1990) Retinal degeneration in the rd mouse is caused by a defect in the β-subunit of rod cGMP-phophodiesterase. Nature 347:677–680.

Caffé AR, Ahuja P, Holmqvist B, Azadi S, Forsell J, Holmqvist I, Söderpalm A, van Veen T (2001a) Mouse retina explants after long term culture in serum free medium. J Chem Neuroanat 22:263–273.

Caffé AR, Sanyal S (1991) Retinal degeneration in vitro: comparison of postnatal retinal development of normal, rd and rds mutant mouse in organ culture. In: Retinal degenerations (Anderson RE, Hollyfield JG, La Vail MM, eds), pp 29–38. Boca Raton: CRC Press, Inc.

Caffé AR, Söderpalm AK, Holmqvist I, van Veen T (2001b) A combination of CNTF and BDNF rescues rd photoreceptors but changes rod differentiation in the presence of RPE in retinal explants. Invest Ophthalmol Vis Sci 42:275–282.

Caffé AR, Söderpalm A, van Veen T (1993) Photoreceptor-specific protein expression of mouse retina in organ culture and retardation of rd degeneration in vitro by a combination of basic fibroblast and nerve growth factors. Curr Eye Res 12:719–726.

Caffé AR, Visser H, Jansen HG, Sanyal S (1989) Histotypic differentiation of neonatal mouse in retina organ culture. Curr Eye Res 8:1083–1092.

Carter-Dawson LD, LaVail MM, Sidman RL (1978) Differential effect of the rd mutation on rods and cones in the mouse retina. Invest Ophthalmol Vis Sci 17:489–498.

Castagné V, Clarke PG (2000) Neuroprotective effects of a new glutathione peroxidase mimetic on neurons of the chicks embryo's retina. J Neurosci Res 59:497–503.

Cho SG, Lee YH, Park HS, Ryoo K, Kang KW, Park J, Eom SJ, Kim MJ, Chang TS, Choi SY, Shim J, Kim Y, Dong MS, Lee MJ, Kim SG, Ichijo H, Choi EJ (2001) Glutathione S-transferase mu modulates the stress-activated signals by suppressing apoptosis signal-regulating kinase 1. J Biol Chem 276:12749–12755.

Coyle JT, Puttfarcken P (1993) Oxidative stress, glutamate, and neurodegenerative disorders. Science 262:689–695.

Götz ME, Kunig G, Riederer P, Youdim MBH (1994) Oxidative stress: free radical production in neural degeneration. Pharmacol Ther 63:37–122.

Grzelak A, Rychlik B, Bartosz G (2000) Reactive oxygen species are formed in cell culture media. Acta Biochim Pol 47:1197–1198.

Halliwell B, Clement MV, Ramalingam J, Long LH (2000) Hydrogen peroxide: ubiquitous in cell culture and in vivo? IUBMB Life 50:251–257.

Hayes JD, Pulford DJ (1995) The glutathione S-transferases supergene family: regulation of GST and the contribution of the isoenzymes to cancer chemoprotection and drug resistance. CRC Crit Rev Biochem Mol Biol 30:445–600.

Holbrook NJ, Ikeyama S (2002) Age-related decline in cellular response to oxidative stress: links to growth factor signaling pathways with common defects. Biochem Pharmacol 64:999–1005.

Jomary C, Neal MJ, Jones SE (2001) Characterization of cell death pathways in murine retinal neurodegeneration implicates cytochrome c release, caspase activation, and bid cleavage. Mol Cell Neurosci 18:335–346.

Joseph JA, Erat S, Denisova N, Villalobos-Molina R (1998) Receptor- and age-selective effects of dopamine oxidation on receptor-G protein interactions in the striatum. Free Radic Biol Med 24: 827–834.

Karlsson K, Lindahl U, Marklund SL (1988) Binding of human extracellular superoxide dismutase C to sulphated glycosaminoglycans. Biochem J 256:29–33.

Knabe W, Ochs M (1999) Horizontal cells invest retinal capillaris in the tree shrew *Tupaia belangeri*. Cell Tissue Res 298:33–43.

Laemmli UK (1970) Cleavage of structural proteins during assembly of the head of bacteriophage T4. Nature 227:680–685.

Leist M, Raab B, Maurer S, Rösick U, Brigelius-Flohe R (1996) Conventional cell culture media do not adequately supply cells with antioxidants and thus facilitate peroxide-induced genotoxicity. Free Radic Biol Med 21:297–306.

Lipton SA, Choi YB, Pan ZH, Lei SZ, Chen HS, Sucher NJ, Loscalzo J, Singel DJ, Stamler JS (1993) A redox-based mechanism for the neuroprotective and neurodestructive effects of nitric oxide and related nitroso-compounds. Nature 364:626–632.

Lovell MA, Xie C, Markesbery WR (1998) Decreased glutathione transferase activity in brain and ventricular fluid in Alzheimer's disease. Neurology 51:1562–1566.

Mannervik B, Danielson UH (1988) Glutathione transferases-structure and catalytic activity. CRC Crit Rev Biochem 23:283–337.

McGuire S, Bostad E, Smith L, Witten M, Siegel FL, Kornguth S (2000) Increased immunoreactivity of glutathione S-transferase in the retina of Swiss Webster mice following inhalation of JP8 +100 aerosol. Arch Toxicol 74:276–280.

McGuire S, Daggett D, Bostad E, Schroeder S, Siegel F, Kornguth S (1996) Cellular localization of glutathione S transferases in retinas of control and lead-treated rats. Invest Ophthalmol Vis Sci 37:833–842.

McLaughlin ME, Ehrhart TL, Berson EL, Dryja TP (1995) Mutation spectrum of the gene encoding the β-subunit of rod phosphodiesterase among patients with autosomal recessive retinitis pigmentosa. Proc Natl Acad Sci USA 92:3249–3253.

Mosinger-Ogilvie J, Speck JD, Lett JM (2000) Growth factors in combination, but not individually, rescue rd photoreceptors in organ culture. Exp Neurol 161:676–685.

Mosinger-Ogilvie J, Speck JD, Lett JM, Fleming TT (1999) A reliable method for organ culture of neonatal mouse retina with long-term survival. J Neurosci Methods 87:57–65.

Mukherjee SB, Aravinda S, Gopalakrishnan B, Nagpal S, Salunke DM (1999) Secretion of glutathione S-transferase isoforms in the seminiferous tubular fluid, tissue distribution and sex steroid binding by rat GSTM1. Biochem J 340:309–320.

Naash MI, Nielsen JC, Anderson RE (1988) Regional distribution of glutathione peroxidase and glutathione S-transferase in adult and premature human retinas. Invest Ophthalmol Vis Sci 29:149–152.

Oury TD, Ho Y-S, Piantadosi CA, Crapo JD (1992) Extracellular superoxide dismutase, nitric oxide, and central nervous system O_2 toxicity. Proc Natl Acad Sci USA 89:9715–9719.

Pittler SJ, Baehr W (1991) Identification of a nonsense mutation in the rod photoreceptor cGMP phosphodiesterase beta-subunit gene of the rd mouse. Proc Natl Acad Sci USA 88:8322–8326.

Pow DV, Crook DK (1995) Immunocytochemical evidence for the presence of high levels of reduced glutathione in radial glial cells and horizontal cells in the rabbit retina. Neurosci Lett 193:25–28.

Puopolo M, Hochstetler SE, Gustincich S, Wightman RM, Raviola E (2001) Extrasynaptic release of dopamine in a retinal neuron: activity dependence and transmitter modulation. Neuron 30:211–225.

Ricart KC, Fiszman ML (2001) Hydrogen peroxide-induced neurotoxicity in cultured cortical cells grown in serum-free and serum-containing media. Neurochem Res 26:801–808.

Salinas AE, Wong MG. Glutathione S-transferases: a review 1999) Curr Med Chem 6:279–309.

Saneto RP, Awasthi YC, Srivastava SK (1982) Glutathione S transferases of the bovine retina. Biochem J 205:213–217.

Sanyal S, Bal AK (1973) Comparative light and electron microscopic study of retinal histogenesis in normal and rd mutant mice. Z Anat Entwicklungsgesch 142:219–238.

Singh SV, Dao DD, Srivastava SK, Awasthi YC (1984) Purification and characterisation of glutathione S-transferases in human retina. Curr Eye Res 3:1273–1280.

Singhal SS, Godley BF, Chandra A, Pandya U, Jin GF, Saini MK, Awasthi S, Awasthi YC (1999) Induction of glutathione S-transferase hGST 5.8 is an early response to oxidative stress in RPE cells. Invest Ophthalmol Vis Sci 40:2652–2659.

Sucher NJ, Lipton SA (1991) Redox modulatory site of the NMDA receptor-channel complex: regulation by oxidized glutathione. J Neurosci Res 30:582–591.

Tanaka K-I, Miyazaki I, Fujita N, Emdadul Haque M, Asanuma M, Ogawa N (2001) Molecular mechanism in activation of glutathione system by ropinirole, a selective dopamine D2 agonist. Neurochem Res 26:31–36.

Yu D-Y, Cringle SJ (2001) Oxygen distribution and consumption within the retina in vascularised and avascular retinas and in animal models of retinal disease. Progr Ret Eye Res 20:175–208.

Yu X, Rajala RV, McGinnis JF, Li F, Anderson RE, Yan X, Li S, Elias RV, Knapp RR, Zhou X, Cao W (2004) Involvement of insulin/phosphoinositide 3-kinase/Akt signal pathway in 17 beta-estradiol-mediated neuroprotection. J Biol Chem 279:13086–13094.

(Accepted 2 November 2004)